PLOS ONE

Hybrid Lentivirus-phiC31-int-NLS Vector Allows Site-Specific Recombination in Murine and Human Cells but Induces DNA Damage

Nicolas Grandchamp[1,2,3], Dorothée Altémir[1,2], Stéphanie Philippe[1,2,3], Suzanna Ursulet[1,2,3], Héloïse Pilet[1,2,3], Marie-Claude Serre[4], Aude Lenain[5], Che Serguera[6], Jacques Mallet[1], Chamsy Sarkis[1,2]*

1 Unit of Biotechnology and Biotherapy, Centre de recherche de l'Institut du Cerveau et de la Moelle Epinière, Pierre-and-Marie-Curie University/Institut National de la Santé et de la Recherche Médicale, Paris, France, 2 NewVectys, Villebon-sur-Yvette, France, 3 Biosource, Paris, France, 4 Laboratoire de Virologie Moléculaire et Structurale, Gif-sur-Yvette, France, 5 Commissariat à l'Energie Atomique, Laboratoire de Radiobiologie et Oncologie, Fontenay-aux-Roses, France, 6 Molecular Imaging Research Center - Modélisation des biothérapies, Fontenay-aux-Roses, France

Abstract

Gene transfer allows transient or permanent genetic modifications of cells for experimental or therapeutic purposes. Gene delivery by HIV-derived lentiviral vector (LV) is highly effective but the risk of insertional mutagenesis is important and the random/uncontrollable integration of the DNA vector can deregulate the cell transcriptional activity. Non Integrative Lentiviral Vectors (NILVs) solve this issue in non-dividing cells, but they do not allow long term expression in dividing cells. In this context, obtaining stable expression while avoiding the problems inherent to unpredictable DNA vector integration requires the ability to control the integration site. One possibility is to use the integrase of phage phiC31 (phiC31-int) which catalyzes efficient site-specific recombination between the *attP* site in the phage genome and the chromosomal *attB* site of its *Streptomyces* host. Previous studies showed that phiC31-int is active in many eukaryotic cells, such as murine or human cells, and directs the integration of a DNA substrate into pseudo *attP* sites (p*attP*) which are homologous to the native *attP* site. In this study, we combined the efficiency of NILV for gene delivery and the specificity of phiC31-int for DNA substrate integration to engineer a hybrid tool for gene transfer with the aim of allowing long term expression in dividing and non-dividing cells preventing genotoxicity. We demonstrated the feasibility to target NILV integration in human and murine p*attP* sites with a dual NILV vectors system: one which delivers phiC31-int, the other which constitute the substrate containing an *attB* site in its DNA sequence. These promising results are however alleviated by the occurrence of significant DNA damages. Further improvements are thus required to prevent chromosomal rearrangements for a therapeutic use of the system. However, its use as a tool for experimental applications such as transgenesis is already applicable.

Background

Gene transfer technologies are essential for genetics studies and gene therapies. However, major challenges remain to be addressed. A major issue is the lack of control over the site of DNA integration in the host genome which leads to unpredictable gene expression level and potentially undesirable mutagenesis of important cellular genes [1]. Recent strategies to tackle this challenge are relying on the use of genome editing tools such as ZFNs [2–7], TALENs [8–13] or more recently CRISPR-Cas system [14–17]. However, the vectorization of these tools into viral vectors to optimize their use *ex vivo* or *in vivo* raises several problems. Indeed, ZFNs function as dimers and generally require cotransduction of three vectors (one for each dimer and one for the recombinating substrate) [18–20]. Moreover ZFNs may induce

cellular toxicity due to off target activity [21–23]. TALENs have an important size with repeat domains hampering their vectorization [24]. CRISPR-Cas is a very recent tool and its vectorization has not yet been described. One may however expect its vectorization into viral vectors will be challenging as the system is based on the concomitant use of a chimeric DNA displaying hairpin structures [25] and of Caspase 9 which induces apoptosis when over-expressed [26]. These features will undoubtedly represent challenges for the vectorization of CRISPR-Cas into viral vectors for targeted integration.

Site-specific recombinases such as Cre [27–34] or FLP [35–38] of the tyrosine recombinases family are other genome editing tools more easily vectorizable and widely used for the purpose of site specific integration. However, the use of these recombinases is limited by the absence of endogenous recognition site in

mammalian cells and by the bidirectionality of the recombination reaction they mediate. Within the superfamily of site-specific recombinases, phage integrases catalyse unidirectional recombination events [39]. Among these the PhiC31 phage integrase (phiC31-int), of the large serine recombinases family, is the most commonly used site-specific integrase for gene transfer purposes [40,41]. In its natural context, phiC31-int mediates efficient recombination between the phage attachment site (attP) and the bacterial attachment site (attB). The recombination of these two sites results in the unidirectional and site-specific integration of the phage genome into the bacterial chromosome (reviewed in [39]) leading to an integrated phage genome flanked by the recombinant attL (left) and attR (right) sites (Figure 1). When used for gene transfer into eukaryotic cells, phiC31-int can catalyse integration of a plasmid containing an attB sequence into endogenous pseudo attP sites (pattP) displaying a high degree of homology with the wild type attP site [42]. Hence, associated with transfection techniques, phiC31-int has been successfully exploited to stably modify the genome into particular genomic sites of many types of eukaryotic cells in vitro [43–50] for transgenesis [48,51–55] and gene therapy applications [56–65]. The use of phiC31-int presents several advantages. First, the recombinase can be used to generate conservative recombination between attB and pseudo attP sites [42]. Second, Chalberg et al demonstrated that the majority of phiC31-int mediated recombination events in the human genome occur in intergenic regions [66]. However, in most of these studies the vectorization of phiC31-int relied on cotransfection (or nucleofection) of plasmids for both the delivery of phiC31-int and of the transgene, thus limiting this technology to in vitro or ex vivo applications.

A strategy to increase the efficiency of DNA delivery in vivo is to use viral-derived vectors. As the expression of the genome editing tool must be transitory to avoid genotoxicity, it could therefore be delivered by a transient viral vector [67]. Even though phiC31-int has already been delivered by an adenoviral vector system [68,69] the use of such vectors is limited by their cell toxicity and immunogenicity [70–72]. In contrast, lentiviral vectors (LV) have the advantage to be non-immunogenic [73,74] and offers the possibility to be pseudotyped by different envelops, allowing a high degree of flexibility regarding the tropism of the particles and the
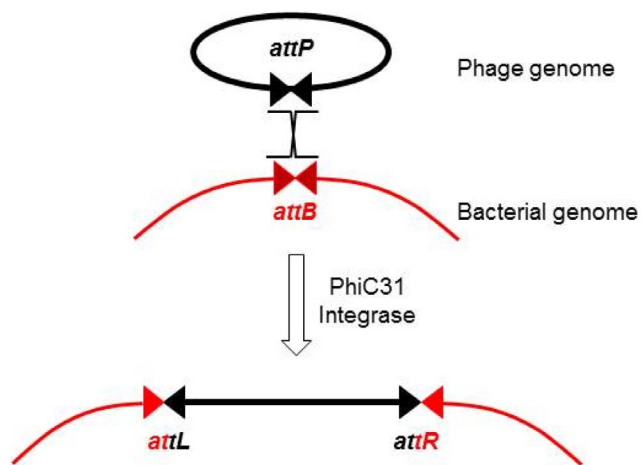
type of cell(s) they transduce (for review see Cronin J. et al [75]). Most importantly, it was shown that LV integrase can be modified to obtain non integrating lentiviral vectors (NILVs) [76–78], which act as episomal vectors. Hence, NILVs are vectors of choice to deliver genome editing tools and have been successfully used to deliver transposases [79,80], FLP [81] or ZFNs [82,83]. However, the use of NILVs has never been described for the vectorization of a serine recombinase.

In the present study, we combine the unidirectional site-specific recombination capability of phiC31-int with the efficiency of NILVs for gene transfer. For targeted integration,two different NILVs, one delivering the DNA sequence to be integrated and containing the natural attB site, the other expressing the phiC31-int are used. Through a step by step approach, we demonstrate for the first time that phiC31-int can be vectorized in NILV and we provide clues to further improve the system. However, analysis of integration events reveals that significant DNA damages can result from phiC31-int mediated recombination. In conclusion, the vectorization of serine recombinases in NILVs is feasible and constitutes a promising tool for basic research; however, one should remain cautious about the chromosomal aberrations that can be induced by these recombinases, particularly for clinical uses.

Results and Discussion

NILV genomes can be used as a substrate for site-specific integration mediated by phiC31-int into human genome

We first assessed the ability of a NILV DNA genome to be used as a substrate for phiC31-int. We therefore generated a Hela cell line constitutively expressing phiC31-int thanks to an integrative lentiviral vector expressing the phiC31-int under the control of the CMV promoter (LV CMV-phiC31-int) to. Hela cells were transduced and clonal populations were isolated and analyzed by RT-PCR to estimate the phiC31-int expression level (Figure 2A). The clone Hi16 was selected for its robust constitutive expression of phiC31-int.

The ability of the constitutively expressed phiC31-int to mediate recombination between a NILV bearing an attB site with genomic pattP sites was then tested. Hi16 cells were transduced with a non-integrative lentiviral vector expressing the Neomycine (Neo) resistance gene under the control of the CMV promoter and containing an attB site (NILV attB-CMV-Neo). After two weeks of G418 selection we obtained four cell clones which genomes were analyzed. Theoretically Neo integration is expected to arise from 3 distinct mechanisms: (i) phiC31-int-**specific** integration, (ii) **residual** integration mediated by a residual activity of the mutant HIV integrase (review about this field [84]) or (iii) **illegitimate** integration due to recombination of the episomal DNA molecule with the cellular genome by host cell mechanisms (Figure 3A). If the analysis is realized with clonal populations, these three different mechanisms should be discriminated by performing 2 PCR assays, one amplifying the LTR and the other amplifying the attB site. A positive LTR PCR reveals the presence of a LTR-LTR junction, indicating that the integration has occurred through a LTR-independent mechanism, either involving attB site-specific recombination or illegitimate recombination. In contrast, a positive attB PCR reveals that the attB site is intact, indicating an attB-independent integration, either involving LTR dependent (residual) integration or illegitimate recombination. In summary, cells are analyzed without knowing whether their genome contains one or several integration of NILV. A positive result for LTR PCR only or for attB PCR only allows to identify the mechanism of integration without ambiguities (ie respectively

Figure 1. Scheme of phiC31-int mediated recombination in bacterial host. PhiC31 integrase performs precise recombination between an attB site located in the Streptomyces genome and an attP site located on the phiC31 phage genome. The outcome is integration of the phage into the host genome.
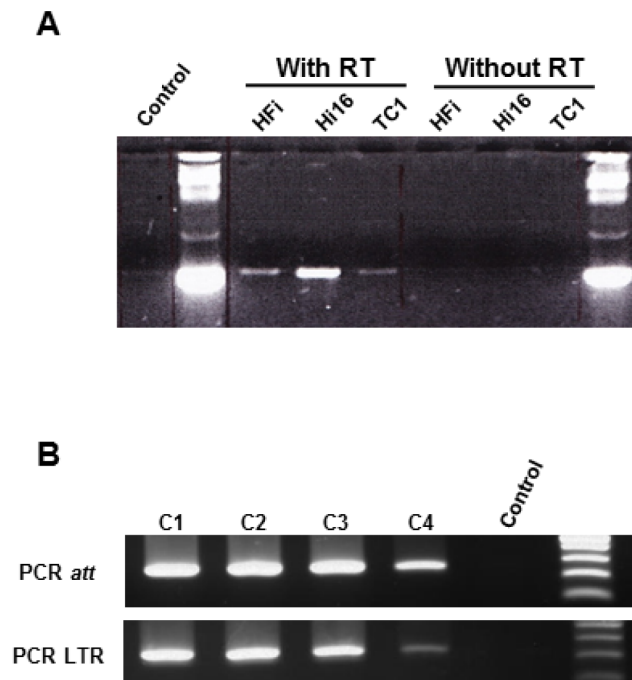doi:10.1371/journal.pone.0099649.g001

A

B

Figure 2. Analysis of cell lines which constitutively expressed phiC31-int. A) PhiC31 RT-PCR on three different cell lines. HFi and Hi16 are derived from Hela cell line and TC1 from NIH-3T3 cell line. Control condition lane lacks RNA. B) PCR which detects LTR junctions or intact *attB* sites after transduction with a NILV *attB*-CMV-Neo.
doi:10.1371/journal.pone.0099649.g002

phic31-int specific integration or residual integration). As the LTR PCR does not amplify the 1-LTR region generated when the linear genome circularized through homologous recombination of both LTR regions, recombination involving 1-LTR circles would always result in LTR− in the PCR test. In cells where a single integration of a 1-LTR circle event arose, attB+/LTR− or attB−/LTR− profiles may be detected, respectively when the recombination is independent or dependent on phiC31-int. In all our experiments, we never observed attB−/LTR− clones. On the contrary, if both PCR are positive integration could result either from illegitimate recombination or from double independent recombination events (ie: phiC31-int site specific recombination and HIV integrase mediated residual integration). We collected the four clones and checked integration pattern of NILV with PCR. The PCR analysis revealed that all clones were positive for both LTR and a*ttB* PCRs (Figure 2B). Thus this result does not allow to conclude about the nature of the integration events.

To clear up this ambiguity, genomic DNA of isolated clones was further analyzed by inverse PCR (iPCR) to isolate potential specific integration events. *attB* based primers (P1/P1′) were used to amplify junctions of recombination. To avoid the PCR background generated by the non-recombined *attB* site, an enzymatic cocktail including an enzyme which cuts only once in the vector sequence, in 5′ to the *attB* site (Figure 3B) was used. In this way, we were able to isolate pseudo *attR* junctions with iPCR, (but not the pseudo *attL* junction). Using this adapted strategy, a lentiviral genome integrated by phiC31-int at the human locus Xq22.1 was detected (Figure 4). Interestingly this locus had already been described as a preferential p*attP* site in the human genome [66]. Moreover, the core sequence is exactly in the same position, suggesting that the recombination event occurred very precisely at this locus.

Although NILV integration also occurred through other means than phiC31-int recombination, our results clearly demonstrate that a NILV is a suitable substrate for phiC31-int mediated recombination in human cells. We therefore investigated whether phiC31-int could function when vectorized in a NILV.

NILVs allow adequate expression of phiC31-int to mediate recombination into a reporter system containing an attP site artificially introduced in human cells

The ability of a NILV to express phiC31-int and mediate recombination between another NILV genome carrying an *attB* site and a wild-type *attP* site artificially introduced in a human cell genome was further tested. First, a clonal Hela cell line containing the wild-type *attP* site inserted in its genome (HDsred line) was generated using an integrative LV (CMV-a*ttP*-DsRED2). HDsred cells were then transduced with two NILVs, one allowing expression of phiC31-int (NILV CMV-phiC31-int), and the other expressing Neo and containing the *attB* site (NILV *attB*-CMV-Neo). After cotransduction cells were grown with G418 to select integration events. The genomic DNA extracted from Neo resistant clones was analyzed by PCR to detect a*ttL* recombination junction (Figure 5A). Results showed only background signal generated by non-recombined *attP* site (figure 5B). To prevent this amplification, the genomic DNA was digested by a restriction enzyme that cuts both *attP* and *attR* sites but not *attL* site (Figure 5A) prior to PCR amplification. PCR results obtained after the enzymatic treatment revealed an a*ttL* junction in the population transduced with the highest dose of phiC31-int vector (Figure 5C). These results have been further confirmed by nested PCR (Figure 5D) and PCR product sequencing. Taken together, these results demonstrate that a NILV can deliver a functional phiC31-int capable to integrate an episomal lentiviral substrate containing an *attB* site into an *attP* site artificially introduced into the human genome.

Although the used PCR strategy does not allow to estimate the targeting efficiency of the *attP* site with the double vector system, the need of a nuclease digestion before PCR to reveal specific integration events suggests that the efficiency of the two NILVs system is low. As this assay involved the two natural recombination sites of PhiC31-int, further reduced efficiency would be expected when targeting endogenous p*attP* sites. Consequently, we next focused on the improvement of the two NILVs system efficiency.

Modification of the phiC31-int sequence to improve the efficiency of the NILV phiC31-int to allow target integration in pseudosites attP

It was previously shown that C-terminal addition of a nuclear localization system (NLS) to phiC31-Int improves its efficiency in eukaryotic cells [85]. We therefore tested this improved integrase in NILV vectorization strategy. To compare the two versions of phiC31-int, Hela cells were cotransduced with the following NILVs vectors: CMV-Neo with or without *attB* site and CMV-phiC31-int with or without NLS. Cells were grown with G418 and the resistant clones were quantified. The results from experiments in which CMV-phiC31-int was cotransduced with either CMV-Neo or *attB*-CMV-Neo are presented in Figure 6A. The CMV-Neo and the *attB*-CMV-Neo conditions did not display significant differences, indicating that no significant PhiC31-int recombinase activity occurred. In contrast, when the cells are transduced with CMV-phiC31-int-NLS instead of CMV-phiC31-Int (Figure 6B) the presence of the NLS sequence induced significant differences between the CMV-Neo and the *attB*-CMV-Neo conditions. These
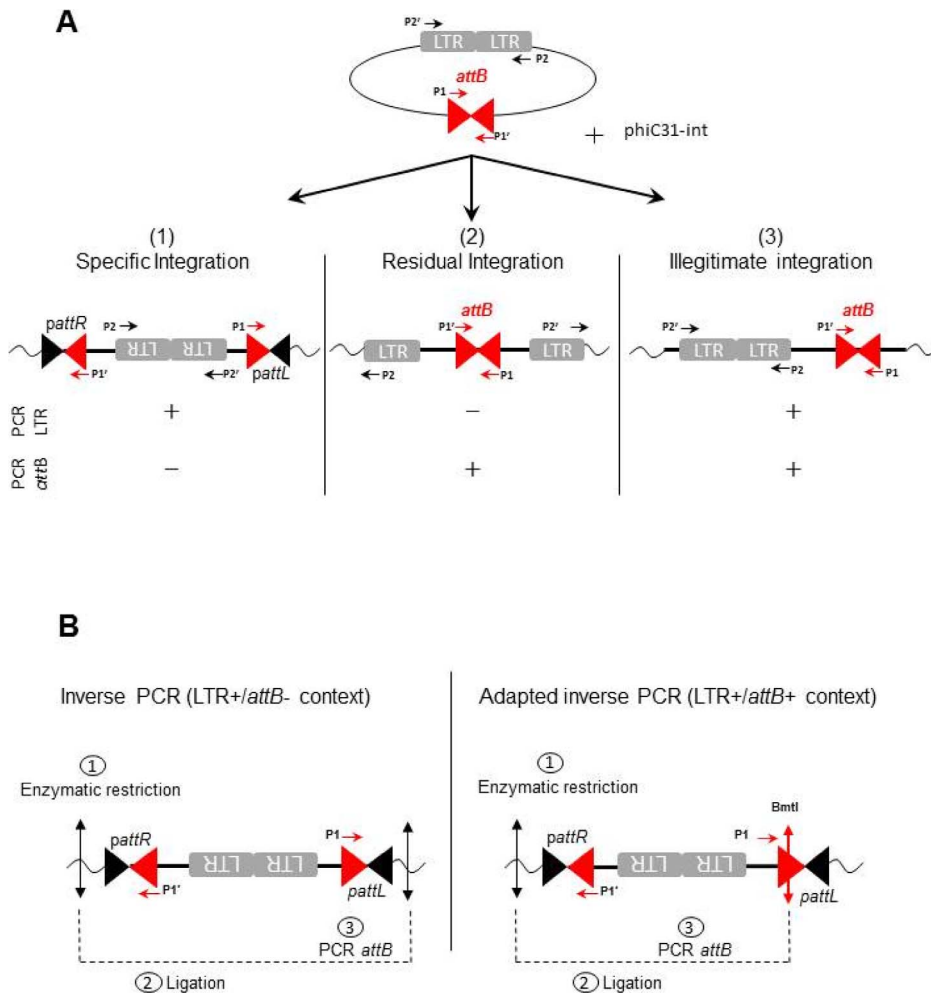
Figure 3. Analysis strategies to detect the specific integrations mediated by phiC31-int. A) Illustration of the three mechanisms of the phiC31-int mediated integration of a NILV containing an *attB* sequence. According to the type of integration, the PCR results in three different profiles: - PCRs LTR+/*attB*− : integration type (1), specific integration. - PCRs LTR−/*attB*+: integration type (2), residual integration. - PCRs LTR+/*attB*+: integration type (3), illegitimate integration. P1/P1′ are the primers used for *attB* PCR and P2/P2′ are the primers used for LTR PCR. B) Schematic representations of the inverse PCR and the adapted inverse PCR strategies used to characterize phiC31-int integration sites. doi:10.1371/journal.pone.0099649.g003

results show that addition of a C-terminal NLS to phiC31-int significantly increased its recombination efficiency with p*attP* sites. Indeed the phiC31-int-NLS mediated integration was 2 to 2.5 fold above the background level produced by NILV residual integration (Figure 6B).

The use of the phiC31-int-NLS vectorized in a NILV allows to significantly increase the efficiency of recombination. We therefore further tested this hybrid lentivirus phiC31-int-NLS vector to target genomic p*attP* site into murine and human cells.

The two NILVs system allows site specific recombination in murine and human cells but induced aberrant chromosomal rearrangements

To target p*attP* site in the murine and human genome with the two vectors system, Hela cells and NIH-3T3 cells were cotransduced with the NILV *attB*-CMV-Neo and the hybrid lentivirus phiC31-int-NLS vector. After two weeks of selection, Neo resistant cells were collected and several clonal populations were isolated to facilitate interpretation of PCR analyses. The clones were analyzed with the LTR and *attB* PCRs assay (Figure 3A) to

determine the proportion of specific integration events compared to NILV residual integration and illegitimate recombination events. We categorized clones in the 3 following groups: LTR+/*attB*− clones (group I, ie phiC31-int-NLS integration), LTR−/*attB*+ clones (group II, ie residual integration) and LTR+/*attB*+ clones (group III, ie illegitimate integration or mixed integration profile). The results are presented in Table 1.

We obtained 108 clones for murine cells and 28 for human cells. 7.5% of murine clones are in group I and 20.3% in group III (Table 1A). Consequently the integration mediated by the hybrid lentivirus phiC31-int-NLS vector is comprised between 7.5% and 27.8%. As no human clone corresponded to group III, the proportion of the hybrid lentivirus phiC31-int-NLS vector specific integration corresponds to the proportion of group I, ie 46.4% (Table 1B).

To determine which integration sites were targeted and confirm the type of integration of clonal groups I and III, we performed an analysis by iPCR as previously described (Figure 3B). The sequencing of iPCR products demonstrates that all human and murine clones tested contain in their genome an integrated vector with a recombinant pattern at the *attB* site. Therefore, the two

A

attB site	TGC CAG GGC GTG CCC **TTG** GGC TCC CCG GGC GCG
attP site	CAA CTG GGG TAA CCT **TTG** AGT TCT CTC AGT TGG
attR site	CAA CTG GGG TAA CCT **TTG** GGC TCC CCG GGC GCG
attL site	TGC CAG GGC GTG CCC **TTG** AGT TCT CTC AGT TGG

B

attB site	TGC CAG GGC GTG CCC **TTG** GGC TCC CCG GGC GCG
Locus Xq22.1	TGC CTC ATT TAA TCT **AT** AGG TTC TCC TTG TTC
Pseudo *attR* site	TGC CTC ATT TAA TCT **TG** GGC TCC CCG GGC GCG

Figure 4. DNA sequence of *att* and p*attP* sites. A) Wild type *attP* and *attB* sites. After recombination two hybrids sites are formed: *attL* and *attR*. B) Recombination between *attB* site and the human locus Xq22.1 This recombination generates a p*attR* which has been isolated by inverse PCR. Xq22.1 had been described previously as a human p*attP* by MP Calos et al., who isolated the same p*attR*.
doi:10.1371/journal.pone.0099649.g004

vectors system that we developed allows targeting p*attP* sites in the murine and human genomes (Table 2).

Twelve murine integration sites were isolated, three from group I with the two junctions (p*attL* and p*attR*) and nine from group III with only the p*attR* junction (Table 2). For two of the three group I clones both flanking regions were sequenced but the isolated junctions were too short to allow identification of the integration locus. Surprisingly, these two clones of group I present abnormal p*attL* and p*attR* junctions where several bases were missing, probably due to a deletion mechanism. Similarly, the sequence analysis of group III clones shows that recombination between the *attB* site and p*attP* site is not as precise as expected. Indeed, 6 out of 9 clones have missing bases in the p*attR* junctions. However, because we isolated only one flanking region for clones of group III, we cannot conclude about deletion events, as the missing bases could result from a gap of the a*attB* core region involved in recombination.

Five human integration sites were isolated, all from group I. Both junctions were isolated for three sites and only the p*attR* junction for two sites (Table 2). As for the murine integration site analysis, missing bases in the recombined pseudo-sites were detected, including in clones for which both L and R junction could be determined. This further confirms that missing bases indeed reveal a deletion mechanism, probably occurring during the phiC31-int mediated recombination between a natural *attB* site and a p*attP* site. Furthermore, the integration site of the three sites for which the two junctions were isolated could be localized exactly (Table 2). Interestingly, for these three sites chromosomal gaps were observed between the p*attR* site and the p*attL* site. The size gaps are 13 bp, 795 pb and 4.8 kbp. The two first gaps could result from a mechanism of deletion which could occur through NHEJ pathway. Nevertheless, these hypotheses cannot explain the

gap of 4.8 kbp. Indeed, in this case, the two flanking regions isolated during iPCR are in the same chromosomal orientation, which is not the case when normal recombination occurs. We hypothesize that the observed aberrant recombination results from two successive recombination events involving two p*attP* sites located 4.8 kb from each other that led to an inversion of the 4.8 kbp sequence (figure 7). This mechanistic model was previously proposed to explain chromosomal rearrangements in mammalian cells resulting from aberrant recombinations mediated by phiC31-int [86].

In conclusion the hybrid lentivirus-phiC31-int-NLS vector that we developed allows targeted integration in p*attP* sites in murine and human genomes but seem to induce frequent deletions of base pairs in the *attB* site present into the vector or into the endogenous p*attP* site. Moreover, it may induce chromosomal deletions and translocations.

Conclusions

Our work establishes the ability of the hybrid lentivirus-phiC31-int-NLS to integrate a NILV substrate into a*attP* or p*attP* sites in murine and human cell lines. Although the number of integration sites isolated in this study does not allow to determine preferential genome recognition sites for integration mediated by phiC31-int vectorized in NILV, a human p*attP* site already described could be isolated [66]. Most importantly, we demonstrated that the use of hybrid lentiviral phiC31-int-NLS vector can induce DNA damages, probably due to the activity of the recombinase. Indeed, other reports already described similar results using non-viral transfection of PhiC31-int. Anja Ehrhardt et al have shown that 15% of transgenes integrated by phiC31-int were flanked by chromosomal DNA sequence from different chromosomes [86]
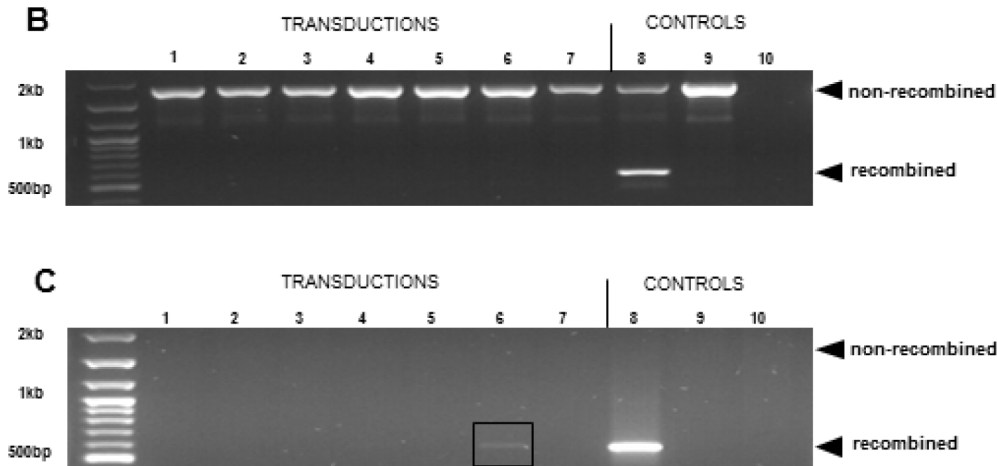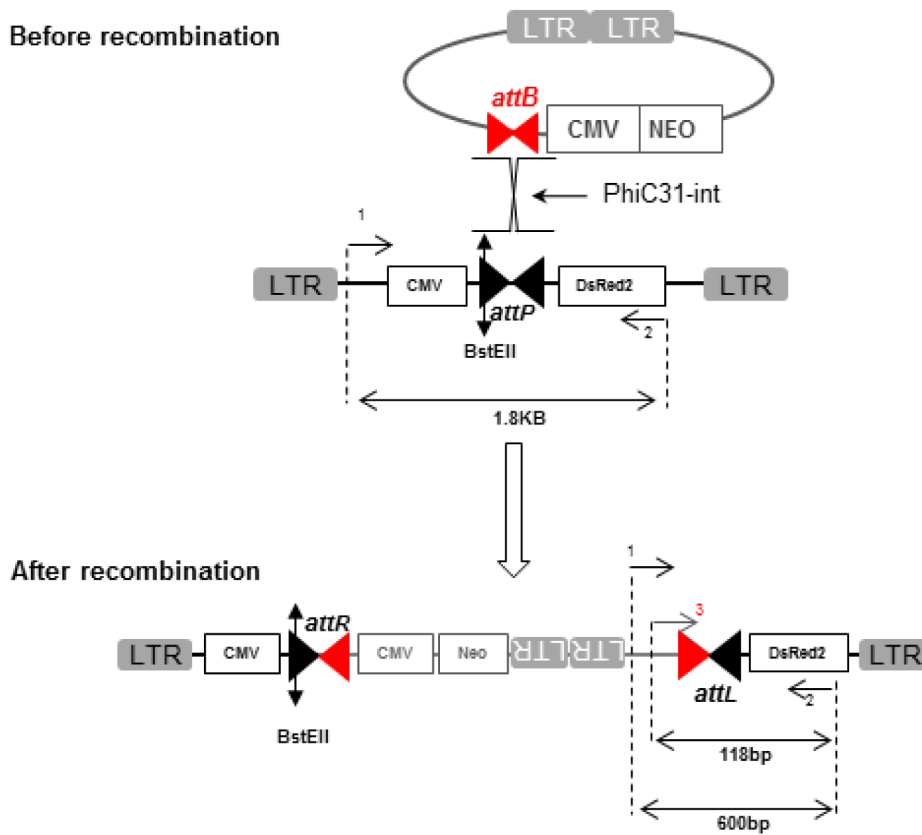
Figure 5. Detection of recombination mediated by phiC31-int between an *attB* site contained into a NILV and a genomic *attP* site. A) Scheme of the DsRed2 PCR before and after the enzymatic restriction treatment. B) PCR DsRed2 results without restriction enzyme treatment. Lanes 1 to 3: cotransduction with CMV-Neo and CMV-PhiC31 increasing vector input of 50–150–300 ng of p24. Lanes 4 to 6: cotransduction with *attB*-CMV-Neo and CMV-PhiC31 increasing vector input of 50–150–300 ng of p24. Lane 7: *attB*-CMV-Neo. Lane 8: positive control generated by triple-transfection (CMV-phiC31-int, *attB*-CMV-Neo and CMV-*attP*-DsRed2). Lane 9: negative control without vector. Lane 10: negative control of PCR. C) PCR DsRed2 results after restriction enzyme treatment. Lanes are similar to figure B. D) Nested PCR from the product isolated from lane 6 to confirm the specificity of PCR DsRed2 amplification.
doi:10.1371/journal.pone.0099649.g005

Figure 6. Effect of NLS sequence on phiC31-int activity in NILV context. A) Cotransduction of NILVs CMV-PhiC31 and CMV-Neo or *attB*-CMV-Neo. Four p24 doses of PhiC31 vector were used (D1: 3 ng, D2: 5 ng, 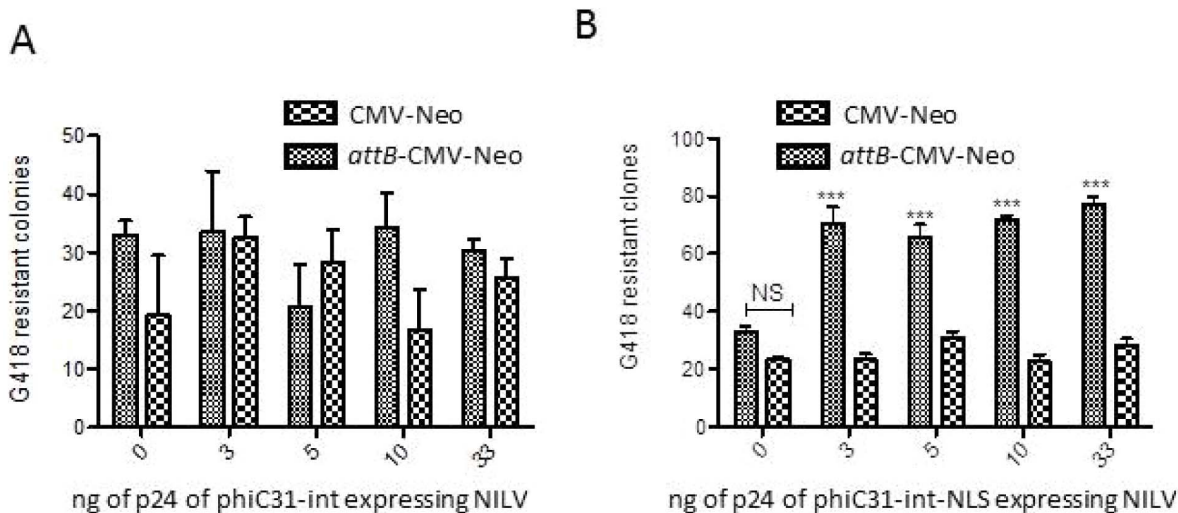D3: 10 ng, D4: 33 ng). B) Cotransduction of NILVs CMV-PhiC31-NLS and CMV-Neo or *attB*-CMV-Neo. Four p24 doses of PhiC31 vector were used (D1: 3 ng, D2: 5 ng, D3: 10 ng, D4: 33 ng). No significant differences are observed between sample with or without *attB* sequence in the vector pTRIP-CMV-Neo. Satistics: two ways ANOVA with Bonferroni posttest (Prism 5).
doi:10.1371/journal.pone.0099649.g006

and Ji Liu et al have shown that phiC31-int induces DNA damages and chromosomal rearrangements in primary and adult human fibroblasts [87,88]. In addition, Ehrard et al. have shown that phiC31-int is competent to integrate linear DNA fragments. They did not characterize the mechanisms and the consequences of this type of event are unknown, but one may hypothesize that such event would induce chromosome break. Considering that the cycle of NILVs involves linear intermediates, it would be of particular interest to further investigate the ability of phiC31-int to integrate these linear forms and the consequences of such events. Taken together, these observations limit the use of the hybrid lentiviral phiC31-int-NLS vector for clinical applications, it remains useful in transgenesis contexts where non aberrant recombination events can be selected. Alternatively, the hybrid lentiviral system may be used to vectorize other recombinases or genome editing tools with higher safety features. Indeed other serine recombinases have been shown to function in human cells [89–91] and could be valuable candidates for vectorization in NILVs. Moreover, the modification of recombinases and other genome editing tools by directed evolution techniques [92,93] could be used to render them hyper-specific and hyper-efficient in order to improve their safety features. For instance, directed evolution has proven efficient to modify the efficiency and/or specify of a variety of molecular tools,

including Sleeping Beauty [94] Cre recombinase [95], FLP recombinase [96], ZFNs [97] or phiC31-int [98].

Methods

Plasmids

The encapsidation plasmid expressing a functional integrase (p8.91 IN_{WT}) has been described previously [77]. The encapsidation plasmid expressing a deficient integrase (p8.91 IN_{D64V}) was derived from the plasmid p8.91 IN_{WT} and the plasmid pCMVΔR(int-)8.2 previously described [74] and kindly provided by D.B. Kohn (UCLA, Los Angeles (CA), USA). This plasmid contains a point mutation in the coding region of the integrase catalytic domain, creating a D64V change in the amino acid sequence. The plasmid p8.91 IN_{D64V} was generated by replacing the BclI-AflII fragment of p8.91 IN_{WT} by the corresponding fragment (containing the substitution) from pCMVΔR(int-)8.2.

The envelope expression plasmid pMDG(VSV) was used to express the VSV-G from the human CMV immediate early promoter [74].

The vector plasmid pTrip-CMV-phic31-int-WPRE was derived from the plasmid pTrip-CMV-GFP-WPRE previously described [77] and the plasmid pCMV-phic31-int previously described [41] and kindly provided by M.P. Calos (Stanford University, Stanford

Table 1. Repartition in 3 groups of human and murine clones according to the *attB* and LTR PCR results.

		Group I (LTR+) *Specific integration*	Group II (attB+) *Residual integration*	Group III (LTR+/attB+) *Unknow integration*
Mouse				
	Clone number	8	78	22
	%	7,5%	72,2%	20,3%
Human				
	Clone number	13	15	0
	%	46,4%	53,6%	0,0%

doi:10.1371/journal.pone.0099649.t001

Table 2. Mapping and description of p*att*P sites isolated by iPCR on human and murine cell lines.

| | | Deletions | | Genomic location | | If intronic | If intergenic, flanking gene names | | | |
| | Number of junction isolated | The half of *att* site present into the vector | Chromosome | Pseudo site | Context | gene name | 5′side gene | Distance (kb) | 3′side gene | Distance (kb) |
Chromosome										
Mouse										
Groupe I										
1	2	p*att*R: 2 bp p*att*L: 42 bp	ND	1E4	repeat sequence					
2	2	p*att*R: No p*att*L: 13 bp	ND	2H3-H4	repeat sequence					
7	2 (only p*att*R exploitable)	p*att*R: 4 bp	ND	7F2 108099955	Exonic	MOR204-16				
Groupe III										
1	1	p*att*R: 8 bp	ND	1H1 159228123	Intergenic		PAPP-A2	277	AI316802	49
5	1	p*att*R: 16 bp	ND	5B1 29812070	Exonic	4632413E21Rik				
5	1	p*att*R : 21 bp	ND	5C31 58057809	Intronic	Pcdh7				
6	1	p*att*R: No	ND	6G1 135251898	Intergenic		Gsg1	7	1700023A18Rik	51
7	1	p*att*R: 4 bp	ND	7A1 7104238	Intergenic		AIE1	90	5730403M16Rik	10
9	1	p*att*R: 12 bp	ND	9A1 3001529	Intronic	AC131780.5-201				
13	1	p*att*R: No	ND	13D1 102691720	Intergenic		AA414921	984	F630107B15	1.5
17	1	p*att*R: No	ND	17A3.3 23698186	Intergenic		EG622645	305	4.1B	53
X	1	p*att*R: 10 bp	ND	XA7.3 75331158	Intronic	Cf-8				
Human										
Groupe I										
1	2	p*att*R: No p*att*L: 20 bp	13 bp	1q32.1 205953621/634	Intergenic		SLC26A9	15	RAB7	28
9	1	p*att*R: 9 bp p*att*L: ND	ND	9p21.1 33615936	Intergenic		bA255A11.3	43	TCRBV20S2	1.5
17	2	p*att*R: No p*att*L: 12 bp	Inversion of 4,8 kb	17q11.2 26164583/59669	Intronic	HSD24				
17	1	p*att*R: No p*att*R: ND	ND	17q21.32 45406611	Intronic	C17orf57				
17	2	p*att*R: 10 bp p*att*L: 34 bp	795 pb	17q25.3 82068091/886	Intergenic		DUS1L	2559	FASN	11080

Step 1 : PhiC31-int mediated NILV integration between *attB* site and p*att1* site
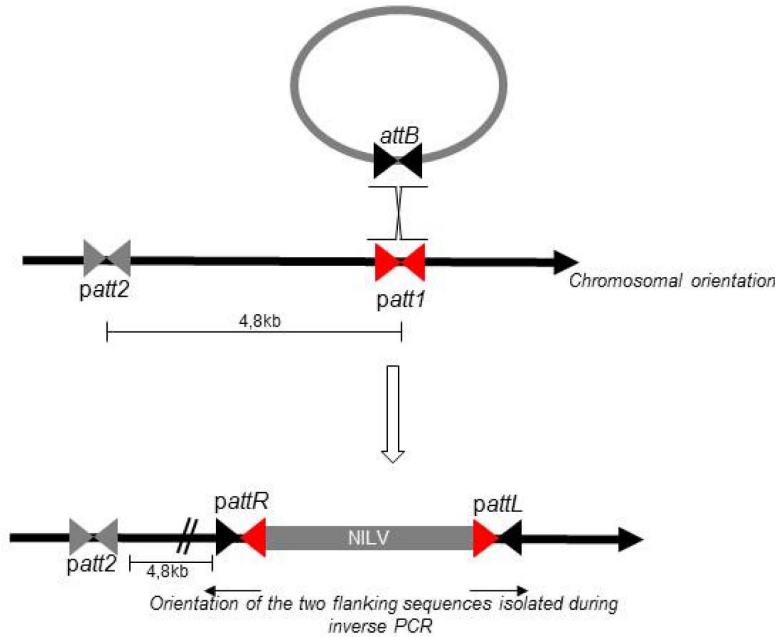
Step 2 : Intramolecular recombination mediated by phiC31-int between the NILV p*attL* site and p*att2* site
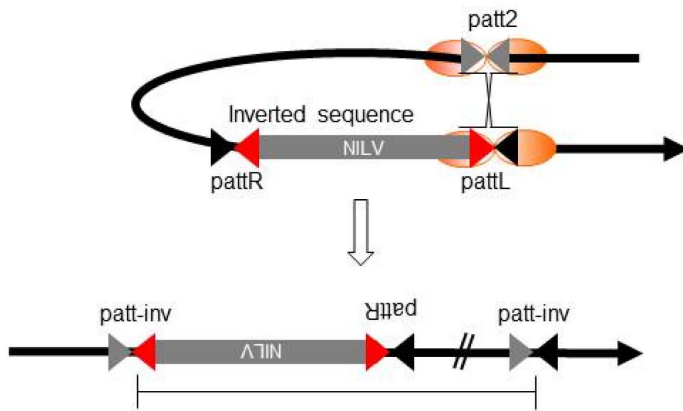

Figure 7. Hypothetical model to explain the inversion of 4.8 Kb detected by iPCR. Step 1: Integration of a NILV mediated by phiC31-int into a p*attP* site. Step2: Recombination mediated by phiC31-int between the p*attL* generated during step 1 and another p*att* site located at 4 kb.
doi:10.1371/journal.pone.0099649.g007

(CA), USA). The plasmid pTrip-CMV-phic31-int-WPRE was generated by replacing the BamHI-SnabI fragment (CMV-GFP) of the pTrip-CMV-GFP-WPRE by the CMV-phic31-int fragment from the plasmid pCMV-phic31-int. The vector plasmid pTrip-CMV-phic31-int-NLS-WPRE was derived from the plasmid pTrip-CMV-phic31-int-WPRE and the plasmid pCMV-phic31-int. The C-terminal region of phic31-int was amplified with a primer containing the SV40 NLS sequence (5′-CCCGTTGGCAGGA-AGCACTTCCGG-3′/5′- ATTCGCGGATCCGCTAAACCT-TCCTCTTCTTCTTAGGCGCCGCTACGTCTTCCGTGCC-GTCC-3′) from the plasmid pCMV-phic31-int. This PCR product was subcloned into the plasmid pCMV-phic31-int in place of the C-terminal region of phic31-int by using Eco47III and BamHI restriction enzymes to generate the plasmid pCMV-phic31-int-NLS. The plasmid pTrip-CMV-phic31-int-NLS-WPRE was finally generated by replacing the SpeI-BamHI fragment (GFP) of the pTrip-CMV-phic31-int-WPRE by the corresponding fragment (phic31-int-NLS) from pCMV-phic31-int-NLS. The vector plasmid pTrip-*attB*-CMV-Neo-WPRE was derived from the plasmid pTrip-CMV-Neo-WPRE previously described [77] and the plasmid p*attB* previously described [41] and kindly provided by MP Calos. The plasmid pTrip-a*ttB*-CMV-Neo-WPRE was generated by inserting the SalI fragment of the p*attB* plasmid (a*ttB* sequence) into the linearized plasmid pTrip-CMV-Neo-WPRE.

The plasmid pTrip-CMV-a*ttP*-DsRed2 was derived from the plasmid pTrip-CMV-DsRed2 kindly provided by P. Ravassard.

Hybridization of 2 single strands DNA fragments (5′- CCCCAA-CTGGGGTAACCTTTGAGTTCTCTCAGTTGGGGG-3′/5′-C-CCCCAACTGAGAGAACTCAAAGGTTACCCCAGTTGGGG-3′) generated a double stranded DNA fragment corresponding to the attP sequence flanked by BamHI cohesive ends. This fragment was inserted into the linearized plasmid pTrip-CMV-attP-DsRed2 to generate the plasmid pTrip-CMV-attP-DsRed2.

Lentiviral production

Lentiviral vectors were generated by the transient transfection of 293T cells by using the calcium phosphate precipitation method previously described [77]. Briefly, cells were cotransfected with the vector plasmid (pTrip-CMV-phic31-int-WPRE, pTrip-CMV-phic31-int-NLS-WPRE, pTrip-attB-CMV-Neo-WPRE or pTrip-CMV-attP-DSred2-WPRE), the transcomplementation plasmid (p8.91 IN_{WT} for integrative vectors or p8.91 IN_{64} for non-integrative vectors), and the plasmid encoding the vesicular stomatitis virus envelope glycoprotein (pMD-G). Supernatant was collected 48 hours after transfection, treated with DNaseI (Roche) and filtered (0.45 μm). Viral particles were then concentrated by ultracentrifugation (90 min, 22,000 rpm, rotor SW28) and resuspended in 0.1M PBS. The HIV p24 Gag antigen was quantified for each stock by ELISA (HIV-1 P24 antigen assay; Beckman Coulter, Fullerton, CA) according to manufacturer's instructions.

Cell culture

Human epithelial HeLa, Hi16, HeLa-DsRED2 and 293T cells and murine NIH 3T3 cells were grown in Dulbecco's modified medium (Invitrogen) supplemented with antibiotics (100 U/mL penicillin and 100 mg/mL streptomycin) and 10% heat inactivated fetal calf serum (Eurobio). The cells were plated and cultured in a humidified incubator at 37°C in a 5% CO2 and 90% air atmosphere.

Genomic DNA extraction

Genomic DNA extractions were performed with a lysis buffer composed of TrisHCl 10 mM (pH 7.5), EDTA 10 mM, SDS 0.6%, RNase A (Qiagen) 100 μg/mL and proteinase K (Eurobio) 100 μg/mL. The lysates were purified by phenol/chloroform and precipitated using sodium acetate and ethanol.

Generation of a reporter cell line HeLa-DsRED2

The HeLa-DsRED2 cell line containing an attP site and expressing DsRED2 fluorescent protein was generated using the lentiviral vector CMV-attP-DsRED2. HeLa cells were transduced with LV CMV-attP-DsRED2 (unconcentrated supernatant). Cells were grown for 3 days and seeded at clonal density in 96-well plates (0.3 cell per well) to generate single cell derived colonies. Clones were analyzed for DsRED2 expression by flow cytometry and PCR amplification of the vector genome.

Transduction

Cell suspensions were incubated for 3 hours with required vectors in medium supplemented with 1 μM DEAE-dextran. After 3 hours of incubation, cells were seed at desired density in fresh medium and grown for the purpose of the experiment.

Hi16 cells (2.10^6 cells/mL) were transduced with NILV-phic31-int (300 ng of p24) and NILV-Neo (100 ng of p24). Cells were seeded in 10 cm plates and grown in medium supplemented with 1 mg/mL of G418 for 12 days. Cells were then seeded in 96 well plates at low density (0.3 cell per well) to generate single cell derived colonies.

HeLa DsRED2 cells (2.10^6 cells/mL) were transduced with NILV CMV-phic31-int (50, 150, 300 ng of p24) and NILV CMV-Neo (100 ng of p24). Cells were seeded in 10 cm plates and grown in medium supplemented with 1 mg/mL of G418 (renewed every 3 days) for 12 days before extraction and analysis of genomic DNA.

Hela and NIH-3T3 cells (5.10^5 cells/mL) were transduced with NILV CMV-phic31-int (300 ng of p24) and NILV CMV-Neo (100 ng of p24). Cells were seeded in 10 cm plates and grown in medium supplemented with 1 mg/mL of G418 for 12 days. Cells were then seeded in 96 well plates at low density (0.3 cell per well) to generate single cell derived colonies.

Evaluation of Recombination Frequency

HeLa were directly transduced in suspension (8.10^4 cells/mL) with NILV CMV-phic31-int (3, 6, 18 and 36 ng of p24) and NILV CMV-Neo (12 ng of p24) during 3 hours in 150 μL of medium supplemented with 1 μM DEAE-dextran. Cells were then seeded in 6-wells plates with 2 mL of fresh medium. The day after, medium was removed and replaced with fresh medium supplemented with 1 mg/mL of G418. The medium was replaced every 3 days. Cells were grown 12 days, until clones developed and were then fixed with PFA 4% and stained with trypan blue. Clones on each well were counted. We transduced cells in three replicate tubes for each condition, and results are expressed as the mean of three measurements.

PCR reactions

RT-PCR. To analyze phic31-int expression by RT-PCR, total RNAs were extracted from HeLa cells using the RNeasy minikit (Qiagen), according to the manufacturer's instructions. Then, RNAs were reverse transcribed using the Superscript First Strand Synthesis kit (Invitrogen), according to the manufacturer's instructions. Phic31-int cDNA was amplified using the primers 5′-GCGAAGATTCTCGACACG-3′ and 5′-TCGCAGTACAGC-TTGTCC-3′ at the concentration of 10 μM.

PCR on genomic DNA. PCR performed on genomic DNA used 500 ng of DNA, 1.5 mM of MgCl2 and 10 μM of each primer. The primers were as follows: amplification of attB region: 5′-CAATTTGCTGAGGGCTATTGAG-3′ and 5′- CTGTCC-CTGTAATAAACCCG-3′; amplification of the LTRs region: 5′-CTCAATAAAGCTTGCCTTGAGTGC-3′ and 5′-TCAGAT-CTGGTCTAACCAGAGAGACC-3′; amplification of the Ds Red2 region: 5′-AGGCCAGACAATTATTGTCTGG-3′ and 5′-ATGGTCTTCTTCTGCATCACG-3′; amplification of DsR ED2 (nested primers) 5′- AAGAATCCTGGCTGTGGAAAG-3′ and 5′-AACTCGGTGATGACGTTCTCG-3′

Inverse PCR. Genomic DNA (10 μg) was primarily submitted to enzymatic restriction. The enzymatic cocktail used was: XbaI (100 U), StuI (100 U) BsrGI (30 U) and BstXI (30 U). After 16 hours incubation, the enzymes were heat inactived at 65°C for 30 minutes. Cohesive ends were filled in with Klenow (15 U) and dNTPs (2 mM) at 25°C for 20 minutes. Klenow was inactived with 1 mM EDTA. The products of digestion were purified by phenol/chloroform and precipitated using sodium acetate and ethanol. The ligation of the digestion products was performed by ligase (1.000 U, NEB) within ligation buffer supplemented with ATP (1 mM). The products of ligation were purified by phenol/chloroform and precipitated using sodium acetate and ethanol. PCR was performed with 100 ng of DNA with primers allowing the amplification of the attB region.

Adapted inverse PCR was performed using the same protocol with the addition of BmtI (30 U) in the enzymatic restriction cocktail.

The products of inverse PCR were visualized on 0.8% agarose gel with ethidium bromide staining. These products were extracted and purified using the Wizard SV Gel and PCR Clean-up System (Promega) according to the manufacturer's instructions, then cloned in a plasmid using pGEM-T Easy Vector System I according to the manufacturer's instructions. Next, inverse PCR products were sequenced using T7 and/or Sp6 primers.

Sequence analysis

All sequencing was performed by Eurofins genomics. Sequences were aligned with vector and genomic DNA, and recombination junctions were identified by sequence matching to a*ttB*. Human and murine blasts were performed using the *NCBI* and *ensembl genome* databases. The chromosomal localization of pseudosites attP has been performed using the Genebank GRCm38.p2

C57BL/6J assembly in mouse and the Primary Assembly GRCh38 for Human.

Author Contributions

Conceived and designed the experiments: NG C. Sarkis. Performed the experiments: NG DA SU HP AL. Analyzed the data: NG C. Sarkis MCS C. Serguera SP. Contributed reagents/materials/analysis tools: NG AL JM. Wrote the paper: NG SP C. Sarkis C. Serguera.

References

1. Hacein-Bey-Abina S, Von Kalle C, Schmidt M, McCormack MP, Wulffraat N, et al. (2003) LMO2-associated clonal T cell proliferation in two patients after gene therapy for SCID-X1. Science 302: 415–419. doi:10.1126/science.1088547

2. Urnov FD, Miller JC, Lee Y-L, Beausejour CM, Rock JM, et al. (2005) Highly efficient endogenous human gene correction using designed zinc-finger nucleases. Nature 435: 646–651. doi:10.1038/nature03556

3. Geurts AM, Cost GJ, Freyvert Y, Zeitler B, Miller JC, et al. (2009) Knockout rats via embryo microinjection of zinc-finger nucleases. Science 325: 433. doi:10.1126/science.1172447

4. Morton J, Davis MW, Jorgensen EM, Carroll D (2006) Induction and repair of zinc-finger nuclease-targeted double-strand breaks in Caenorhabditis elegans somatic cells. Proc Natl Acad Sci U S A 103: 16370–16375. doi:10.1073/pnas.0605633103

5. Bozas A, Beumer KJ, Trautman JK, Carroll D (2009) Genetic analysis of zinc-finger nuclease-induced gene targeting in Drosophila. Genetics 182: 641–651. doi:10.1534/genetics.109.101329

6. Hockemeyer D, Soldner F, Beard C, Gao Q, Mitalipova M, et al. (2009) Efficient targeting of expressed and silent genes in human ESCs and iPSCs using zinc-finger nucleases. Nat Biotechnol 27: 851–857. doi:10.1038/nbt.1562

7. Gaj T, Guo J, Kato Y, Sirk SJ, Barbas CF 3rd (2012) Targeted gene knockout by direct delivery of zinc-finger nuclease proteins. Nat Methods 9: 805–807. doi:10.1038/nmeth.2030

8. Boch J, Scholze H, Schornack S, Landgraf A, Hahn S, et al. (2009) Breaking the code of DNA binding specificity of TAL-type III effectors. Science 326: 1509–1512. doi:10.1126/science.1178811

9. Moscou MJ, Bogdanove AJ (2009) A simple cipher governs DNA recognition by TAL effectors. Science 326: 1501. doi:10.1126/science.1178817

10. Tesson L, Usal C, Ménoret S, Leung E, Niles BJ, et al. (2011) Knockout rats generated by embryo microinjection of TALENs. Nat Biotechnol 29: 695–696. doi:10.1038/nbt.1940

11. Carlson DF, Tan W, Lillico SG, Stverakova D, Proudfoot C, et al. (2012) Efficient TALEN-mediated gene knockout in livestock. Proc Natl Acad Sci U S A 109: 17382–17387. doi:10.1073/pnas.1211446109

12. Sander JD, Cade L, Khayter C, Reyon D, Peterson RT, et al. (2011) Targeted gene disruption in somatic zebrafish cells using engineered TALENs. Nat Biotechnol 29: 697–698. doi:10.1038/nbt.1934

13. Hockemeyer D, Wang H, Kiani S, Lai CS, Gao Q, et al. (2011) Genetic engineering of human pluripotent cells using TALE nucleases. Nat Biotechnol 29: 731–734. doi:10.1038/nbt.1927

14. Cho SW, Kim S, Kim JM, Kim J-S (2013) Targeted genome engineering in human cells with the Cas9 RNA-guided endonuclease. Nat Biotechnol 31: 230–232. doi:10.1038/nbt.2507

15. Mali P, Yang L, Esvelt KM, Aach J, Guell M, et al. (2013) RNA-guided human genome engineering via Cas9. Science 339: 823–826. doi:10.1126/science.1232033

16. Friedland AE, Tzur YB, Esvelt KM, Colaiácovo MP, Church GM, et al. (2013) Heritable genome editing in C. elegans via a CRISPR-Cas9 system. Nat Methods. doi:10.1038/nmeth.2532

17. Hwang WY, Fu Y, Reyon D, Maeder ML, Tsai SQ, et al. (2013) Efficient genome editing in zebrafish using a CRISPR-Cas system. Nat Biotechnol 31: 227–229. doi:10.1038/nbt.2501

18. Bitinaite J, Wah DA, Aggarwal AK, Schildkraut I (1998) FokI dimerization is required for DNA cleavage. Proc Natl Acad Sci U S A 95: 10570–10575.

19. Wah DA, Bitinaite J, Schildkraut I, Aggarwal AK (1998) Structure of FokI has implications for DNA cleavage. Proc Natl Acad Sci U S A 95: 10564–10569.

20. Smith J, Bibikova M, Whitby FG, Reddy AR, Chandrasegaran S, et al. (2000) Requirements for double-strand cleavage by chimeric restriction enzymes with zinc finger DNA-recognition domains. Nucleic Acids Res 28: 3361–3369.

21. Pruett-Miller SM, Reading DW, Porter SN, Porteus MH (2009) Attenuation of zinc finger nuclease toxicity by small-molecule regulation of protein levels. PLoS Genet 5: e1000376. doi:10.1371/journal.pgen.1000376

22. Cornu TI, Cathomen T (2010) Quantification of zinc finger nuclease-associated toxicity. Methods Mol Biol Clifton NJ 649: 237–245. doi:10.1007/978-1-60761-753-2_14

23. Ramalingam S, Kandavelou K, Rajenderan R, Chandrasegaran S (2011) Creating designed zinc-finger nucleases with minimal cytotoxicity. J Mol Biol 405: 630–641. doi:10.1016/j.jmb.2010.10.043

24. Holkers M, Maggio I, Liu J, Janssen JM, Miselli F, et al. (2013) Differential integrity of TALE nuclease genes following adenoviral and lentiviral vector gene transfer into human cells. Nucleic Acids Res 41: e63. doi:10.1093/nar/gks1446

25. Jore MM, Lundgren M, van Duijn E, Bultema JB, Westra ER, et al. (2011) Structural basis for CRISPR RNA-guided DNA recognition by Cascade. Nat Struct Mol Biol 18: 529–536. doi:10.1038/nsmb.2019

26. Druskovic M, Suput D, Milisav I (2006) Overexpression of caspase-9 triggers its activation and apoptosis in vitro. Croat Med J 47: 832–840.

27. Orban PC, Chui D, Marth JD (1992) Tissue- and site-specific DNA recombination in transgenic mice. Proc Natl Acad Sci U S A 89: 6861–6865.

28. Smith AJ, De Sousa MA, Kwabi-Addo B, Heppell-Parton A, Impey H, et al. (1995) A site-directed chromosomal translocation induced in embryonic stem cells by Cre-loxP recombination. Nat Genet 9: 376–385. doi:10.1038/ng0495-376

29. Tsien JZ, Chen DF, Gerber D, Tom C, Mercer EH, et al. (1996) Subregion- and cell type-restricted gene knockout in mouse brain. Cell 87: 1317–1326.

30. Rohlmann A, Gotthardt M, Willnow TE, Hammer RE, Herz J (1996) Sustained somatic gene inactivation by viral transfer of Cre recombinase. Nat Biotechnol 14: 1562–1565. doi:10.1038/nbt1196-1562

31. Pfeifer A, Brandon EP, Kootstra N, Gage FH, Verma IM (2001) Delivery of the Cre recombinase by a self-deleting lentiviral vector: efficient gene targeting in vivo. Proc Natl Acad Sci U S A 98: 11450–11455. doi:10.1073/pnas.201415498

32. Marumoto T, Tashiro A, Friedmann-Morvinski D, Scadeng M, Soda Y, et al. (2009) Development of a novel mouse glioma model using lentiviral vectors. Nat Med 15: 110–116. doi:10.1038/nm.1863

33. DuPage M, Dooley AL, Jacks T (2009) Conditional mouse lung cancer models using adenoviral or lentiviral delivery of Cre recombinase. Nat Protoc 4: 1064–1072. doi:10.1038/nprot.2009.95

34. Anton M, Graham FL (1995) Site-specific recombination mediated by an adenovirus vector expressing the Cre recombinase protein: a molecular switch for control of gene expression. J Virol 69: 4600–4606.

35. O'Gorman S, Fox DT, Wahl GM (1991) Recombinase-mediated gene activation and site-specific integration in mammalian cells. Science 251: 1351–1355.

36. Moldt B, Staunstrup NH, Jakobsen M, Yáñez-Muñoz RJ, Mikkelsen JG (2008) Genomic insertion of lentiviral DNA circles directed by the yeast Flp recombinase. BMC Biotechnol 8: 60. doi:10.1186/1472-6750-8-60

37. Nakano M, Odaka K, Ishimura M, Kondo S, Tachikawa N, et al. (2001) Efficient gene activation in cultured mammalian cells mediated by FLP recombinase-expressing recombinant adenovirus. Nucleic Acids Res 29: E40.

38. Kondo S, Takata Y, Nakano M, Saito I, Kanegae Y (2009) Activities of various FLP recombinases expressed by adenovirus vectors in mammalian cells. J Mol Biol 390: 221–230. doi:10.1016/j.jmb.2009.04.057

39. Smith MCM, Brown WRA, McEwan AR, Rowley PA (2010) Site-specific recombination by phiC31 integrase and other large serine recombinases. Biochem Soc Trans 38: 388–394. doi:10.1042/BST0380388

40. Thorpe HM, Smith MC (1998) In vitro site-specific integration of bacteriophage DNA catalyzed by a recombinase of the resolvase/invertase family. Proc Natl Acad Sci U S A 95: 5505–5510.

41. Groth AC, Olivares EC, Thyagarajan B, Calos MP (2000) A phage integrase directs efficient site-specific integration in human cells. Proc Natl Acad Sci U S A 97: 5995–6000. doi:10.1073/pnas.090527097

42. Thyagarajan B, Olivares EC, Hollis RP, Ginsburg DS, Calos MP (2001) Site-specific genomic integration in mammalian cells mediated by phage phiC31 integrase. Mol Cell Biol 21: 3926–3934. doi:10.1128/MCB.21.12.3926-3934.2001

43. Belteki G, Gertsenstein M, Ow DW, Nagy A (2003) Site-specific cassette exchange and germline transmission with mouse ES cells expressing phiC31 integrase. Nat Biotechnol 21: 321–324. doi:10.1038/nbt787

44. Nakayama G, Kawaguchi Y, Koga K, Kusakabe T (2006) Site-specific gene integration in cultured silkworm cells mediated by phiC31 integrase. Mol Genet Genomics MGG 275: 1–8. doi:10.1007/s00438-005-0026-3

45. Ishikawa Y, Tanaka N, Murakami K, Uchiyama T, Kumaki S, et al. (2006) Phage phiC31 integrase-mediated genomic integration of the common cytokine receptor gamma chain in human T-cell lines. J Gene Med 8: 646–653. doi:10.1002/jgm.891

46. Ma Q, Sheng H, Yan J, Cheng S, Huang Y, et al. (2006) Identification of pseudo attP sites for phage phiC31 integrase in bovine genome. Biochem Biophys Res Commun 345: 984–988. doi:10.1016/j.bbrc.2006.04.145

47. Thyagarajan B, Liu Y, Shin S, Lakshmipathy U, Scheyhing K, et al. (2008) Creation of engineered human embryonic stem cell lines using phiC31 integrase. Stem Cells Dayt Ohio 26: 119–126. doi:10.1634/stemcells.2007-0283

48. Lister JA (2011) Use of phage φC31 integrase as a tool for zebrafish genome manipulation. Methods Cell Biol 104: 195–208. doi:10.1016/B978-0-12-374814-0.00011-2

49. Groth AC, Fish M, Nusse R, Calos MP (2004) Construction of transgenic Drosophila by using the site-specific integrase from phage phiC31. Genetics 166: 1775–1782.

50. Allen BG, Weeks DL (2005) Transgenic Xenopus laevis embryos can be generated using phiC31 integrase. Nat Methods 2: 975–979. doi:10.1038/nmeth814.

51. Allen BG, Weeks DL (2006) Using phiC31 integrase to make transgenic Xenopus laevis embryos. Nat Protoc 1: 1248–1257. doi:10.1038/nprot.2006.183.

52. Meredith JM, Underhill A, McArthur CC, Eggleston P (2013) Next-generation site-directed transgenesis in the malaria vector mosquito Anopheles gambiae: self-docking strains expressing germline-specific phiC31 integrase. PLoS One 8: e59264. doi:10.1371/journal.pone.0059264

53. Fish MP, Groth AC, Calos MP, Nusse R (2007) Creating transgenic Drosophila by microinjecting the site-specific phiC31 integrase mRNA and a transgene-containing donor plasmid. Nat Protoc 2: 2325–2331. doi:10.1038/nprot.2007.328

54. Bischof J, Maeda RK, Hediger M, Karch F, Basler K (2007) An optimized transgenesis system for Drosophila using germ-line-specific phiC31 integrases. Proc Natl Acad Sci U S A 104: 3312–3317. doi:10.1073/pnas.0611511104

55. Hollis RP, Stoll SM, Sclimenti CR, Lin J, Chen-Tsai Y, et al. (2003) Phage integrases for the construction and manipulation of transgenic mammals. Reprod Biol Endocrinol RBE 1: 79. doi:10.1186/1477-7827-1-79

56. Bertoni C, Jarrahian S, Wheeler TM, Li Y, Olivares EC, et al. (2006) Enhancement of plasmid-mediated gene therapy for muscular dystrophy by directed plasmid integration. Proc Natl Acad Sci U S A 103: 419–424. doi:10.1073/pnas.0504505102

57. Ortiz-Urda S, Thyagarajan B, Keene DR, Lin Q, Calos MP, et al. (2003) PhiC31 integrase-mediated nonviral genetic correction of junctional epidermolysis bullosa. Hum Gene Ther 14: 923–928. doi:10.1089/104303403765701204

58. Olivares EC, Hollis RP, Chalberg TW, Meuse L, Kay MA, et al. (2002) Site-specific genomic integration produces therapeutic Factor IX levels in mice. Nat Biotechnol 20: 1124–1128. doi:10.1038/nbt753

59. Bauer JW, Laimer M (2004) Gene therapy of epidermolysis bullosa. Expert Opin Biol Ther 4: 1435–1443. doi:10.1517/14712598.4.9.1435

60. Held PK, Olivares EC, Aguilar CP, Finegold M, Calos MP, et al. (2005) In vivo correction of murine hereditary tyrosinemia type I by phiC31 integrase-mediated gene delivery. Mol Ther J Am Soc Gene Ther 11: 399–408. doi:10.1016/j.ymthe.2004.11.001

61. Chalberg TW, Genise HL, Vollrath D, Calos MP (2005) phiC31 integrase confers genomic integration and long-term transgene expression in rat retina. Invest Ophthalmol Vis Sci 46: 2140–2146. doi:10.1167/iovs.04-1252

62. Chavez CL, Keravala A, Chu JN, Farruggio AP, Cuéllar VE, et al. (2012) Long-term expression of human coagulation factor VIII in a tolerant mouse model using the φC31 integrase system. Hum Gene Ther 23: 390–398. doi:10.1089/hum.2011.110

63. Keravala A, Portlock JL, Nash JA, Vitrant DG, Robbins PD, et al. (2006) PhiC31 integrase mediates integration in cultured synovial cells and enhances gene expression in rabbit joints. J Gene Med 8: 1008–1017. doi:10.1002/jgm.928

64. Portlock JL, Keravala A, Bertoni C, Lee S, Rando TA, et al. (2006) Long-term increase in mVEGF164 in mouse hindlimb muscle mediated by phage phiC31 integrase after nonviral DNA delivery. Hum Gene Ther 17: 871–876. doi:10.1089/hum.2006.17.871

65. Keravala A, Chavez CL, Hu G, Woodard LE, Monahan PE, et al. (2011) Long-term phenotypic correction in factor IX knockout mice by using ΦC31 integrase-mediated gene therapy. Gene Ther 18: 842–848. doi:10.1038/gt.2011.31

66. Chalberg TW, Portlock JL, Olivares EC, Thyagarajan B, Kirby PJ, et al. (2006) Integration specificity of phage phiC31 integrase in the human genome. J Mol Biol 357: 28–48. doi:10.1016/j.jmb.2005.11.098

67. Wilson JH (2003) Pointing fingers at the limiting step in gene targeting. Nat Biotechnol 21: 759–760. doi:10.1038/nbt0703-759

68. Ehrhardt A, Yant SR, Giering JC, Xu H, Engler JA, et al. (2007) Somatic integration from an adenoviral hybrid vector into a hot spot in mouse liver results in persistent transgene expression levels in vivo. Mol Ther J Am Soc Gene Ther 15: 146–156. doi:10.1038/sj.mt.6300011

69. Robert M-A, Zeng Y, Raymond B, Desfossé L, Mairey E, et al. (2012) Efficacy and site-specificity of adenoviral vector integration mediated by the phage φC31 integrase. Hum Gene Ther Methods 23: 393–407. doi:10.1089/hgtb.2012.122

70. Raper SE, Chirmule N, Lee FS, Wivel NA, Bagg A, et al. (2003) Fatal systemic inflammatory response syndrome in a ornithine transcarbamylase deficient patient following adenoviral gene transfer. Mol Genet Metab 80: 148–158.

71. Schnell MA, Zhang Y, Tazelaar J, Gao GP, Yu QC, et al. (2001) Activation of innate immunity in nonhuman primates following intraportal administration of adenoviral vectors. Mol Ther J Am Soc Gene Ther 3: 708–722. doi:10.1006/mthe.2001.0330

72. Byrnes AP, Rusby JE, Wood MJ, Charlton HM (1995) Adenovirus gene transfer causes inflammation in the brain. Neuroscience 66: 1015–1024.

73. Kafri T, Blömer U, Peterson DA, Gage FH, Verma IM (1997) Sustained expression of genes directly into liver and muscle by lentiviral vectors. Nat Genet 17: 314–317. doi:10.1038/ng1197-314

74. Naldini L, Blömer U, Gallay P, Ory D, Mulligan R, et al. (1996) In vivo gene delivery and stable transduction of nondividing cells by a lentiviral vector. Science 272: 263–267.

75. Cronin J, Zhang X-Y, Reiser J (2005) Altering the tropism of lentiviral vectors through pseudotyping. Curr Gene Ther 5: 387–398.

76. Yáñez-Muñoz RJ, Balaggan KS, MacNeil A, Howe SJ, Schmidt M, et al. (2006) Effective gene therapy with nonintegrating lentiviral vectors. Nat Med 12: 348–353. doi:10.1038/nm1365

77. Philippe S, Sarkis C, Barkats M, Mammeri H, Ladroue C, et al. (2006) Lentiviral vectors with a defective integrase allow efficient and sustained transgene expression in vitro and in vivo. Proc Natl Acad Sci U S A 103: 17684–17689. doi:10.1073/pnas.0606197103

78. Grandchamp N, Henriot D, Philippe S, Amar L, Ursulet S, et al. (2011) Influence of insulators on transgene expression from integrating and non-integrating lentiviral vectors. Genet Vaccines Ther 9: 1. doi:10.1186/1479-0556-9-1

79. Vink CA, Gaspar HB, Gabriel R, Schmidt M, McIvor RS, et al. (2009) Sleeping beauty transposition from nonintegrating lentivirus. Mol Ther J Am Soc Gene Ther 17: 1197–1204. doi:10.1038/mt.2009.94

80. Staunstrup NH, Moldt B, Mátés L, Villesen P, Jakobsen M, et al. (2009) Hybrid lentivirus-transposon vectors with a random integration profile in human cells. Mol Ther J Am Soc Gene Ther 17: 1205–1214. doi:10.1038/mt.2009.10

81. Moldt B, Staunstrup NH, Jakobsen M, Yáñez-Muñoz RJ, Mikkelsen JG (2008) Genomic insertion of lentiviral DNA circles directed by the yeast Flp recombinase. BMC Biotechnol 8: 60. doi:10.1186/1472-6750-8-60

82. Cornu TI, Cathomen T (2007) Targeted genome modifications using integrase-deficient lentiviral vectors. Mol Ther J Am Soc Gene Ther 15: 2107–2113. doi:10.1038/sj.mt.6300345

83. Lombardo A, Genovese P, Beausejour CM, Colleoni S, Lee Y-L, et al. (2007) Gene editing in human stem cells using zinc finger nucleases and integrase-defective lentiviral vector delivery. Nat Biotechnol 25: 1298–1306. doi:10.1038/nbt1353

84. Sarkis C, Philippe S, Mallet J, Serguera C (2008) Non-integrating lentiviral vectors. Curr Gene Ther 8: 430–437.

85. Andreas S, Schwenk F, Küter-Luks B, Faust N, Kühn R (2002) Enhanced efficiency through nuclear localization signal fusion on phage PhiC31-integrase: activity comparison with Cre and FLPe recombinase in mammalian cells. Nucleic Acids Res 30: 2299–2306.

86. Ehrhardt A, Engler JA, Xu H, Cherry AM, Kay MA (2006) Molecular analysis of chromosomal rearrangements in mammalian cells after phiC31-mediated integration. Hum Gene Ther 17: 1077–1094. doi:10.1089/hum.2006.17.1077

87. Liu J, Skjørringe T, Gjetting T, Jensen TG (2009) PhiC31 integrase induces a DNA damage response and chromosomal rearrangements in human adult fibroblasts. BMC Biotechnol 9: 31. doi:10.1186/1472-6750-9-31

88. Liu J, Jeppesen I, Nielsen K, Jensen TG (2006) Phi c31 integrase induces chromosomal aberrations in primary human fibroblasts. Gene Ther 13: 1188–1190. doi:10.1038/sj.gt.3302789

89. Gregory MA, Till R, Smith MCM (2003) Integration site for Streptomyces phage phiBT1 and development of site-specific integrating vectors. J Bacteriol 185: 5320–5323.

90. Kolot M, Meroz A, Yagil E (2003) Site-specific recombination in human cells catalyzed by the wild-type integrase protein of coliphage HK022. Biotechnol Bioeng 84: 56–60. doi:10.1002/bit.10747

91. Olivares EC, Hollis RP, Calos MP (2001) Phage R4 integrase mediates site-specific integration in human cells. Gene 278: 167–176.

92. Miller OJ, Bernath K, Agresti JJ, Amitai G, Kelly BT, et al. (2006) Directed evolution by in vitro compartmentalization. Nat Methods 3: 561–570. doi:10.1038/nmeth897

93. Tay Y, Ho C, Droge P, Ghadessy FJ (2010) Selection of bacteriophage lambda integrases with altered recombination specificity by in vitro compartmentalization. Nucleic Acids Res 38: e25. doi:10.1093/nar/gkp1089

94. Zayed H, Izsvák Z, Walisko O, Ivics Z (2004) Development of hyperactive sleeping beauty transposon vectors by mutational analysis. Mol Ther J Am Soc Gene Ther 9: 292–304. doi:10.1016/j.ymthe.2003.11.024

95. Santoro SW, Schultz PG (2002) Directed evolution of the site specificity of Cre recombinase. Proc Natl Acad Sci U S A 99: 4185–4190. doi:10.1073/pnas.022039799

96. Bolusani S, Ma C-H, Paek A, Konieczka JH, Jayaram M, et al. (2006) Evolution of variants of yeast site-specific recombinase Flp that utilize native genomic sequences as recombination target sites. Nucleic Acids Res 34: 5259–5269. doi:10.1093/nar/gkl548

97. Guo J, Gaj T, Barbas III CF (2010) Directed Evolution of an Enhanced and Highly Efficient FokI Cleavage Domain for Zinc Finger Nucleases. J Mol Biol 400: 96–107. doi:10.1016/j.jmb.2010.04.060

98. Sclimenti CR, Thyagarajan B, Calos MP (2001) Directed evolution of a recombinase for improved genomic integration at a native human sequence. Nucleic Acids Res 29: 5044–5051.